Electronic Supplementary Information

Direct Conversion of Lignocellulosic Biomass to Biomimetic Tendril-Like Functional Carbon Helices: A Protein Friendly Host for Cytochrome C

Kanakaraj Aruchamy,[a] Meena Bisht,[b] P. Venkatesu,[b] D. Kalpana,[c] Nidhi M. R,[a] Nripat Singh,[d] Debasis Ghosh,[a] Dibyendu Mondal,[*a] and Sanna Kotrappanavar Nataraj [*a]

[a]Centre for Nano & Material science, Jain Global Campus, Jain University, Bangalore 562112, India. *Corresponding author, *e-mail: sk.nataraj@jainuniversity.ac.in; sknata@gmail.com; m.dibyendu@jainuniversity.ac.in; dmtapu@gmail.com

[b]Department of Chemistry, University of Delhi, Delhi – 110 007, India.

[c]Central Electrochemical Research Institute -Madras unit, CSIR Madras Complex, Taramani, Chennai - 600 113.

[d]Natural Products & Green Chemistry Division, CSIR-Central Salt & Marine Chemicals Research Institute, Gijubhai Badheka Marg, Bhavnagar 364002, Gujarat, India

Experimental Procedures

Materials

Choline chloride and anhydrous Ferric chloride ($FeCl_3$) was purchased from S.D. Fine Chemicals, Mumbai, India and used without any further purification. *Parthenium hysterophorous* and *Ricinus communis* plants (biomass) has been collected in and around the Jain University campus (35°8'7.80' N, 106°31'9.97 W), Bangalore, Karnataka, India. Cotton was purchased from Medplus medical shop, Bangalore, India. Silk cocoon from *Bombyx mori* were received from the silkworm harvesting farmers from the Yeduvanahalli village, Ramanagara, India. Cytochrome C (Cyt C) from equine heart with purity >95%, hydrogen peroxide solution (H_2O_2) 30 % (w/w) in H_2O, 2, 2-azino-bis (3-ethylbenzothiazoline-6-sulfonic acid) (ABTS) with purity >98% and D_2O, were purchased from Sigma Aldrich, USA. Hydrochloric acid (HCl, 38%) and Ethanol (C_2H_6O, 99.9%) were purchased from S D Fine-Chem Ltd. India and Changshu Hongsheng Fine Chemicals Co. Ltd. China, respectively. Laboratory produced double distilled water was used throughout the process.

Pre-treatment of biomass

Parthenium hysterophorous (uniquely called as congress grass in India), which is abundantly available throughout the year in many countries such as China, Pacific Islands, Australia and India with major weed status, **reported as a natural enemy (noxious weed) because of its effects on crop production, animal husbandry, human health and biodiversity**.[1] Hence it is imperative to completely remove these biomass to stabilize the crop production and environment health. By considering the properties of *Parthenium hysterophorous* such as fast growth rate, high reproductive potential, adaptive nature and, interference by resource depletion, in a positive way a successful establishment of these weed can be a great achievement in weed management.[2] There are few works reported, where researchers used this *Parthenium hysterophorous* for the synthesis of activated carbon to the removal of dyes and heavy metal ions (Cd (II), Hg (II)) from wastewater.[3-6]

Table S1. CHNS data of different parts of raw biomass after dried in oven at 100 °C for overnight.

Sample	C (%)	H (%)	N (%)	S (%)
Parthenium hysterophorous stems	37.3	5.8	1.7	0.1
Parthenium hysterophorous flowers	39.3	5.9	3.5	0.3
Parthenium hysterophorous leaves	40.7	6.1	4.3	0.3
Ricinus communis leaves	44.6	6.3	3.8	0.27
Cotton	40.7	4.9	0.00	0.00
Silk cocoon from Bombix mori	43.1	5.8	5.5	0.0

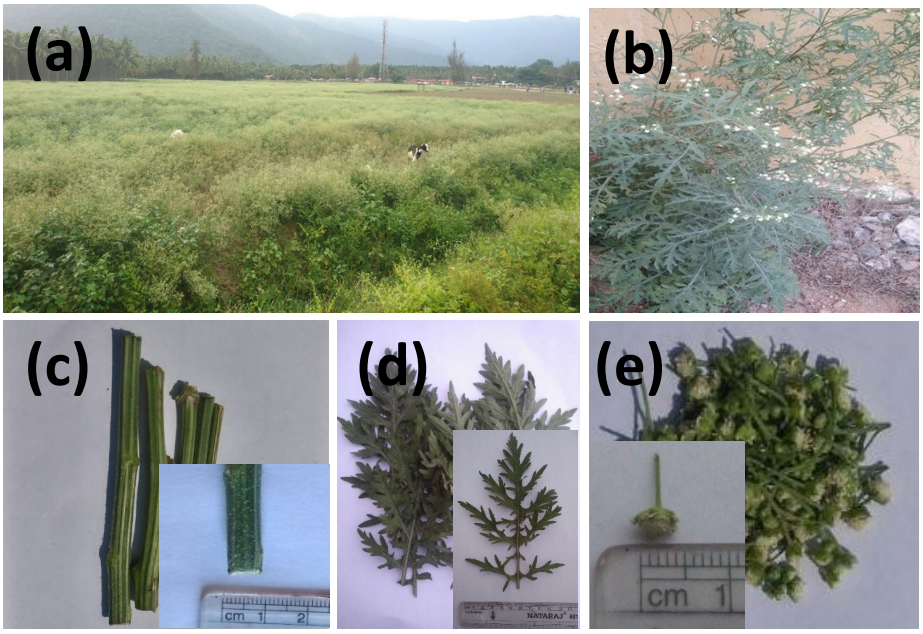

Figure S1. Photographs of *Parthenium Hysterophorous* plant. (a) Acres of agriculture land occupied by *Parthenium hysterophorous* in outer part of the city of Coimbatore, Tamilnadu, India (11.0168° N, 76.9558° E), (b) Individual plant from roadsides, (c) Separated Stems, (d) Leaves and (e) Flowers of *the* plant.

All the leaves, stems, and flowers of *Parthenium hysterophorous* were divided separately and dried in hot air oven at 105 °C for overnight and grounded to micron sized particles. Then to study the chemical compositions, samples were characterized using CHNS analysis and the results indicated that that comparing flowers and stems, leaves were higher in carbon, hydrogen, nitrogen and sulfur content (Table S1). Therefore, all the further work carried out only using leaves of the biomass. Figure S1 shows the photographs of *Parthenium hysterophorous and its different parts.*

Preparation of Deep Eutectic Solvents (DESs)

DES was prepared as per earlier report.[7] In a typical procedure, required amount of choline chloride (CC) and $FeCl_3$ in a 1:2 molar ratio, respectively, was taken in a round bottom flask and the mixture was heated on a hot plate at 80 °C for 2h with continuous stirring until a viscous semi-liquid mixture is formed. This mixture was collected and the moisture content was found to be 8-10 wt%. This CC-$FeCl_3$ (1:2 molar ratios) was used as DES for the solvothermal treatment of the biomass as discuss below.

Solvothermal treatment of the Parthenium hysterophorous

(i) **In presence of water only:** For the control study of conversion of *Parthenium hysterophorous* to carbon with water, 5g of *Parthenium hysterophorous* leaves powder and 50 mL of double distilled water was taken in a sealed vessel of Teflon lined stainless steel autoclave and hydrothermally treated at 200 °C for 18 hrs. After the completion of solvothermal treatment, the autoclave was allowed to cool down to room temperature. The hydrothermal carbon was collected and filtered through Whatman filter paper and washed at least 3 times with 1M HCl solution to remove the metal ions impurities. After that the remaining materials was washed with plenty of double distilled water to remove the acid from the carbon materials followed by washing again with 4:6 ratio of ethanol :

water. Finally the carbon materials was collected and dried in a hot air oven at 80 °C for overnight to obtain fine powder.

(ii) **In presence of water and choline chloride:** To study the effect of only choline chloride a control study of conversion of *Parthenium hysterophorous* to solvothermal carbon with water and choline chloride was conducted. 7.5g of *Parthenium hysterophorous* leaves powder was added to 5g of choline chloride and mixed thoroughly by a glass rod and was heated at 80 °C for 1 h to prepare a solid mixture. Afterwards, 5g of this solid mixture and 50 mL of double distilled water was taken in a sealed vessel of Teflon lined stainless steel autoclave and hydrothermally treated at 200 °C for 18 hrs. After the completion of solvothermal treatment, the autoclave was allowed to cool down to room temperature. The dark-brown color solution was collected and filtered through Whatman filter paper and washed 3 times with 1M HCl solution to remove the metal ions impurities. After that the remaining material was washed with double distilled water to remove the acid from the carbon materials followed by washing again with 4:6 ratio of ethanol:water. Finally the carbon materials was collected and dried in a hot air oven at 80 °C for overnight to obtain fine powder.

(iii) **In presence of water and $FeCl_3$:** To understand the effect of only $FeCl_3$ a control experiment of conversion of *Parthenium hysterophorous* to solvothermal carbon with water and $FeCl_3$ was conducted. The procedure is similar as above experiment (ii).

(iv) **In presence of water and DES:** Preparation of tendrils-like functionalized carbon helices was prepared by solvothermal method employing mixture of DES and water. 7.5g of *Parthenium hysterophorous* leaves powder was added to the 15g of CC-$FeCl_3$ (1:2 molar ratio) and mixed thoroughly by a glass rod and was heated at 80 °C for 1 hr to prepare a solid mixture. Afterwards, 5g of this solid mixture and 50 mL of double distilled water was taken in an air leak free sealed vessel of Teflon lined stainless steel autoclave and solvothermally treated at various temperatures (150-250 °C) and timings (6-24 hrs). After the completion of solvothermal treatment, the autoclave was allowed to cool down to room temperature. The dark-brown color solution was collected and filtered through Whatman filter paper and washed at least 3 times with 1M HCl solution to remove the metal ions impurities. After that the remaining materials was washed with double distilled water to remove the acid from the carbon materials followed by washing with 4:6 ratio of ethanol : water. Finally the carbon materials was collected and dried in a hot air oven at 80 °C for overnight to obtain fine powder. The yields of the final products were calculated following the equation as: Yield = $(W/W_0) \times 100$, wherein, W is the weight of final product and W_0 is the weight of biomass taken initially. The yield was found to be in the range of 42-72%. The details of sample codes and their reaction conditions are provided in Table S2.

Solvothermal treatment of (i) Ricinus communis (ii) Cotton and (iii) Bombyx mori

The possibilities for the formation of helical morphology from different cellulose and lignocellulose biomass by hydrothermal/solvothermal method was studied for (i) *Ricinus communis* leaves which is lignocellulosic biomass (25-45% cellulose + 25-50% hemicellulose + 15-40% lignin) (ii) *Cotton* which is a Cellulosic biomass (99% cellulose) and (iii) *Bombyx mori* which is mainly composed of Fibroin(75%) and Sericin(22.5%) proteins.

(i) ***Solvothermal treatment of Ricinus communis:*** 7.5g of *Ricinus communis* leaves powder was added to the 15g of CC-$FeCl_3$ (1:2 molar ratio) of DES and mixed thoroughly by a glass rod and was heated at 80 °C for 1 hr to prepare a solid mixture. Afterwards, 5g of this solid mixture and 50 mL of double

distilled water was taken in an air leak free sealed vessel of Teflon lined stainless steel autoclave and solvothermally treated at 200 °C for 18hrs. After the completion of solvothermal treatment, the autoclave was allowed to cool down to room temperature. The dark-brown color solution was collected and filtered through Whatman filter paper and washed at least 3 times with 1M HCl solution to remove the metal ions impurities. After that the remaining materials was washed with double distilled water to remove the acid from the carbon materials followed by washing with 4:6 ratio of ethanol : water. Finally the carbon materials was collected and dried in a hot air oven at 80 °C for overnight to obtain fine powder. The yields of the final products were calculated following the equation as: Yield = (W/W_0) x 100, wherein, W is the weight of final product and W_0 is the weight of biomass taken initially. The yield details has given in Table 5.

(ii) ***Solvothermal treatment of Cotton:*** 7.5g of *Cotton* was added to the 15g of CC-$FeCl_3$ (1:2 molar ratio) of DES and mixed thoroughly by a glass rod and was heated at 80 °C for 1 hr to prepare a solid mixture. Afterwards, 5g of this solid mixture and 50 mL of double distilled water was taken in an air leak free sealed vessel of Teflon lined stainless steel autoclave and solvothermally treated at 200 °C for 18hrs. The similar procedure was followed for washing and drying to achieve the final product as mentioned in the above experiment (i).

(iii) ***Solvothermal treatment of Bombyx mori:*** 7.5g of *Bombyx mori* was added to the 15g of CC-$FeCl_3$ (1:2 molar ratio) of DES and mixed thoroughly by a glass rod and was heated at 80 °C for 1 hr to prepare a solid mixture. Afterwards, 5g of this solid mixture and 50 mL of double distilled water was taken in an air leak free sealed vessel of Teflon lined stainless steel autoclave and solvothermally treated at 200 °C for 18hrs. The similar procedure was followed for washing and drying to achieve the final product as mentioned in the above experiment (i).

Table S2. Sample coding of hydrothermally /solvothermally treated *Parthenium hysterophorous* in different conditions

S. No	Sample Code	Conditions
1	Control	*Parthenium hysterophororous* leaves + water treated at 200 °C for 18 hours
2	Control-CC	*Parthenium hysterophororous* leaves + Water + CC treated at 200 °C for 18 hours
3	Control-Fe	*Parthenium hysterophororous* leaves + water + $FeCl_3$ treated at 200 °C for 18 hours
4	PH-18-150	*Parthenium hysterophororous* leaves + Water + DESs treated at 150 °C for 18 hours
5	PH-18-180	*Parthenium hysterophororous* leaves + Water + DESs treated at 180 °C for 18 hours
6	PH-18-200	*Parthenium hysterophororous* leaves + Water + DESs treated at 200 °C for 18 hours
7	PH-18-220	*Parthenium hysterophororous* leaves + Water + DESs treated at 220 °C for 18 hours
8	PH-18-250	*Parthenium hysterophororous* leaves + Water + DESs treated at 250 °C for 18 hours
9	PH-6-200	*Parthenium hysterophororous* leaves + Water + DESs treated at 200 °C for 6 hours
10	PH-12-200	*Parthenium hysterophororous* leaves + Water + DESs treated at 200 °C for 12 hours
11	PH-24-200	*Parthenium hysterophororous* leaves + Water + DESs treated at 200 °C for 24 hours
12	RC-18-200	*Recinus communis* leaves + Water + DESs treated at 200 °C for 18 hours
13	Cotton-18-200	*Cotton* + Water + DESs treated at 200 °C for 18 hours
14	BM-18-200	*Silk cocoon from Bombyx mori* + Water + DESs treated at 200 °C for 18 hours

Reusability study of Solvent

The reusability of the solvent was studied by reusing the solvent which is recovered after the hydrothermal reaction. In a typical procedure, after the hydrothermal method the solvent and the solute separated by filtration using wattman filter paper. The amount of solvent recovered was 45mL, with that 5mL of double distilled water was added to equalize the solvent loss during the hydrothermal treatment. Afterwards 1.7g of *parthenium hysterophorous* (*PH*) leaves powder was added to the solvent and mixed by a magnetic stirrer for 10 mins to acquire a uniform mixture. The same procedure was repeated for two times to examine the reusability of solvent for the next two cycles. The reproducibility of the helical carbon was confirmed in each cycle of the reused solvent which is verified by images of FE-SEM (Figure S3). The yield was calculated by considering the initial amount of *Parthenium hysterophourous* leaves powder which is used for the reaction as 100%. The yield observed second and third cycle was 40.0% and 37.7 % respectively.

Determination of extractable compounds content from pristine PH-18-200

The *PH* powder after hydrothermal treatment separated by filtration, and used without further washing for the calculation of extractable compounds content. The extractable from hydrothermally treated *PH* powder was studied for different solvents such as (i) Water (ii) Ethanol (iii) 1:1 Water: Ethanol mixture and (iv) Dichloromethane. For the experiment 50 mL of the above mentioned different solvents have been taken in four different beakers separately. 100 mg of hydrothermally treated *PH* powder was added on each beaker and stirred

using a magnetic stirrer for 24 hrs in ambient conditions. Afterwards, the solvent with the solute filtered, dried and extractable were calculated. The details of extractable given in **Table S3.**

Table S3. Extractable from PH-18-200 using different solvents.

Extractable (mg/g)			
Water	Ethanol	1:1 (water: Ethanol)	Di-chloromethane
113	134	191	78

Peroxidase activity of Cyt C in presence of carbon helices

The peroxidase activity of the Cyt C was measured using ABTS as substrate in the presence of H_2O_2. Cyt C catalyzes the oxidation of ABTS in the presence of H_2O_2 and produces the green-colored $ABTS^+$ radical. The formation of the $ABTS^+$ radical was monitored by changes in the absorption spectra at 420 nm. The absorption spectra were acquired for mixtures containing 2 µM of Cyt C, 3 mM of ABTS, 1mM of H_2O_2 and different functional carbon helices. The concentration of stock solution of carbon material was 10 mg/mL and 10 uL of this stock solution was used for 600 µL sample. The reaction was initiated with the addition of H_2O_2. The reaction was subjected to 1 min of incubation with continuous measurements of absorbance changes at 420 nm. Relative activity was calculated considering 100% of enzyme activity in water.

Methods

Characterization of carbon helices

The chemical compositions of samples were characterized using CHNS instrument Elementar Vario EL III. Ash content of the carbon samples was calculated by subtracting the amount before and after the calcination of samples in air at 550 ^oC for 2 hrs in a muffle furnace. The crystallinity were analyzed using powder X-ray diffraction (RIGAKU) operating with Cu–Kα1 radiation (l = 1.54 A˚) at scan rate of 3° min^{-1} and a 2 theta range of 5-60°. The crystal index of cellulose were calculated using the formula, Crystal Index = $[(I_{22.1^\circ} - I_{16^\circ})/ I_{22.1^\circ}]*100$. [8] The surface morphology and the size of the samples were studied using Field emission scanning electron microscopy (FESEM) using JSM-7100F. To study the functional groups of the samples ATR-IR (BRUKER) spectra were recorded using 4000-600 cm^{-1}. To study the chemical structure of the samples solid state CP MAS ^{13}C MAS-NMR spectra were recorded on Bruker 500 MHz Advance II spectrometer with 4 mm MAS 1H/BB probe. To study structural fingerprint Raman spectra were recorded by instrument model LabRAM HR Evolution of HORIBA using CCD and InGaAs detectors with automated laser switching source of 514 nm. To quantitatively analyze the elemental composition of samples X-ray photoelectron spectra also were carried out by Thermo Scientific instrument model ESCALAB 250XI BASE SYSTEM WITH UPS AND XPS IMAGE MAPPING using sources of XR6 Micro-focused Monochromator (Al K_α XPS) XR4 Twin Anode Mg/Al (300/400W) X-Ray Source, and EX06 Ion gun for a total acquisition time of 54.5 secs with a Pass energy of 150 eV and energy step size of 1 eV. Stress-strain property (stress and elongation at break) of carrageenan based films were determined using Zwick Roell Z2.5 UTM instrument, with 10 mm/min crosshead speed. The testXpert II-V3.5 software was used for data analysis at room temperature. Current-voltage (I–V) measurements were performed using a Keithley 2635A source meter unit (SMU).

Investigation of the stability of Cyt C in the presence of carbon helices

The stability of Cyt C in presence of different carbon material was studied by UV-visible, Fourier transform infrared (FTIR) and circular dichrosim (CD) spectroscopies. UV-Vis spectra of the Cyt C in the absence and presence of various solvothermal carbons were recorded using a Shimadzu UV-1800 (Japan) spectrophotometer with the highest resolution (1 nm) using matched 1 cm path length quartz cuvettes. CD spectroscopic studies were performed using a Jasco-1500 spectrophotometer, equipped with a Peltier system for temperature control. CD calibration was performed using (1S)-(+)-10-camphorsulphonic acid (Aldrich, Milwaukee, WI), which exhibits a 34.5 M/cm molar extinction coefficient at 285 nm and 2.36 M/cm molar ellipticity (Θ) at 295 nm. The sample was pre-equilibrated at 25 ^{o}C for 25-30 min and the 100 scan speed was fixed for adaptive sampling (accuracy of + 0.01) with a response time of 1s and 1 nm bandwidth. Far-UV and near-UV CD spectra were monitored in the range 190–250 nm and 350–450 nm in cuvette with path length of 0.1 cm and 1 cm, respectively. All spectra were averaged of three scans. Each sample spectrum was obtained by subtracting the appropriate blank media from the experimental spectrum and was collected by averaging three spectra. The concentration of Cyt C was 10 µM for UV and CD analysis. FTIR spectra of Cyt C in the absence and presence of various solvothermal carbons were recorded by using a thermo scientific FTIR spectrometer. Samples were held in an IR cells with ZnSe windows and 15 µm path length teflon spacer. 256 scans were performed at 4 cm^{-1} resolution and averaged. All samples were prepared in D_2O with 5mg/mL concentration of the Cyt C and equilibrated for 2 hrs to facilitate H-D exchange in the protein sample. To be able to compare the effect of various solvothermal carbons, a proper subtraction of D_2O was carried out from each sample. The concentration of stock solution of carbon material was 10 mg/mL and 10 uL of this stock solution was used for 600 µL sample. All the solvothermal carbon materials were dispersed using an ultrasonicator for 3 hrs in water prior to the experiment.

Experimental Results

Importance of carbon helices and limitation of their preparation

There are many diversity of structures of carbon has been fabricated such as diamond-like,[9] nanotubes,[10] onions,[11] fullerenes,[12] nanohorns,[13] straight carbon fibers,[14] and helix-shaped carbon fibers[15] which provides the flexibility to tailor their properties for various potential applications such as catalyst,[16] water purification,[17] energy storage,[18] and agriculture.[19] **A significant efforts have been made for the synthesis of helical carbons due to the unique morphology and applications in different fields such as adsorption that can induce an electrical current and a magnetic field which can be used in microwave absorbers,[20] sensors,[21] and actuators[22].** Many methods has been introduced for the synthesis of carbon springs such as (1) Ni catalyzed DC plasma enhanced chemical vapor deposition (CVD) processes[23] (2) Fe-catalytic pyrolysis of various hydrocarbons such as acetylene, ethylene and propylene, etc., in the temperature range of 650-800 °C[24] (3) CVD using acetylene as a carbon source and copper nanoparticles as catalysts and heat treating at 900 °C for 1 hr.[20]

Table S4. Literatures reported for the preparation of carbon with helical morphology

S. No	Precursor	Method	Catalyst	Condition	Morphology	References
1	Acetylene	CVD	Cu-catalyzed	250 °C for 30mins under vacuum	Carbon helical nanofibers	[15]
2	Acetylene	CVD	Copper tartrate	271 °C for 10mins at atmospheric pressure	Twin helical nanofibers	[26]
3	Acetylene and H_2	CVD	Ni-Xerogel catalyzed	450 °C for 1 hr at atmospheric pressure	Carbon nanocoils	[25]
4	Acetylene, H_2 and Ar	CVD	Ag nanoparticles	450 °C for 15 mins at atmospheric pressure	Carbon nanocoils	[27]
5	Acetylene	CVD	Alkali catalysts	500-700 °C for 1 hr under vacuum	Carbon helical nanofibers	[28]
6	Commercial acetone, H_2 and Ar	CVD	Ni powder	550–800 °C at atmospheric pressure	Double and triple stranded carbon micro-coils	[29]
7	Acetylene, H_2 and N_2	Fluidized bed reactor	$NiSO_4/Al_2O_3$	650 °C	Twisted carbon fibers	[30]
8	Acetylene and Ar	CVD	Stainless steel plates	700 °C for 30 mins at atmospheric pressure	Carbon nanocoils	[31]
9	Acetylene and NH_3	DC plasma enhanced CVD	Ni catalyst	780 °C	CNT with zig zag morphology	[23]
10	Acetylene and He	CVD	Fe–Mg–Co–Sn catalyst	700 °C for 15 mins	Carbon nanocoils	[24]
11	Acetylene and Ar	CVD	Sn–Fe Catalyst	710 °C	Carbon nanocoils	[32]
12	Zucchini	Pyrolysis	Fe(III)	650 °C for 3 hrs under nitrogen flow	Carbon microcoils	[33]
13	Acetylene and Ar	CVD	$Fe_2(SO_4)_3/SnCl_2$	710 °C for 30 mins	Carbon nanocoils	[21]
14	Acetylene	CVD	Cu nanoparticles	900 °C for 1 hr	Carbon nanocoils	[20]
15	Acetylene	CVD	Absolute ethanol and nickel nitrate	750 °C for 15 mins	Carbon nanocoils	[34]
16	*Parthenium hystrophorous* (biomass)	Hydrothermal method	DESs	150-250 °C for 6-24 hrs	Tendril like functionalized carbon helices	Present work

Till now, the minimum temperature used for the formation of carbon micro springs is higher than 450 °C where C_2H_2 and H_2 (or) Ar employed as the source gas and Ni-xerogel (or) Ag nanopartilcles as catalyst by chemical vapor deposition method.[25] **Table S4 summarizes the different protocols highlighting the process conditions such as carbon precursors, methods, catalyst used and reaction conditions.**

CHNS analysis

The elemental compositions of carbon, hydrogen and nitrogen have been studied using a CHNS data analysis and the data are provided in Table S5. From the CHNS analyses a gradual decrease in all the C, H, N and S content were observed with increasing the temperature of the solvothermal process. Moreover in the case of increasing the time duration of the reaction by keeping the temperature of 200 °C as constant all the C, H, N and S contents were decreased. Finally the results conclude that the content of C, H, N, and S were corresponds to the reaction conditions.

Table S5. Yields, ash contents, and elemental compositions of carbon materials prepared under various conditions.

Sample	C (%)	H (%)	N (%)	S (%)	Ash (%)	Yield (%)
PH-18-150	38.51	6.18	1.59	6.19	1.60	72.03
PH-18-180	41.51	6.99	1.65	6.40	2.40	66.03
PH-18-200	36.91	6.72	1.39	3.37	2.80	48.02
PH-18-220	36.51	6.74	1.28	5.93	2.40	45.02
PH-18-250	31.98	6.03	1.23	5.67	1.60	42.02
PH-6-200	37.72	7.49	1.21	8.19	0.80	66.03
PH-12-200	37.10	7.40	1.34	8.83	1.60	54.03
PH-24-200	36.55	7.00	1.17	4.73	2.00	46.03
RC-18-200	69.68	6.45	0.00	0.00	0.6	24.4
Cotton-18-200	66.51	7.28	0.00	0.00	0.4	10.96
BM-18-200	64.24	5.81	0.50	0.00	3.2	2.81

Field Emission Scanning Electron Microscopy (FESEM)

The morphology changes of carbon samples prepared at different conditions were studied using field emission scanning electron microscopy (FESEM). Typically the samples were optimized with different conditions (Figure S2) by solvothermal method. In the solvent optimization process $FeCl_3$ and choline chloride have been used as control whereas there were no traces for the formation of carbon springs in the case of Control-CC. But in case of controll-Fe the formation of carbon helics were found in some cases, however with an incomplete structure. At low time duration (PH-6-200) formation of some carbon spring was observed, however the morphology was not uniform. At high time durations such as PH-12-200 non-uniformity and incomplete forms of carbon springs, and for conditions of PH-24-200 the broken forms of carbon helices were obtained. The prepared carbon helices had a helical diameter of 8 to 9 microns and a fiber diameter of 1.5-2 microns respectively. On the basis of these results we can conclude that it's not only the catalyst (Fe) that helps the formation of carbon helices but also the reaction parameters of the solvothermal process.

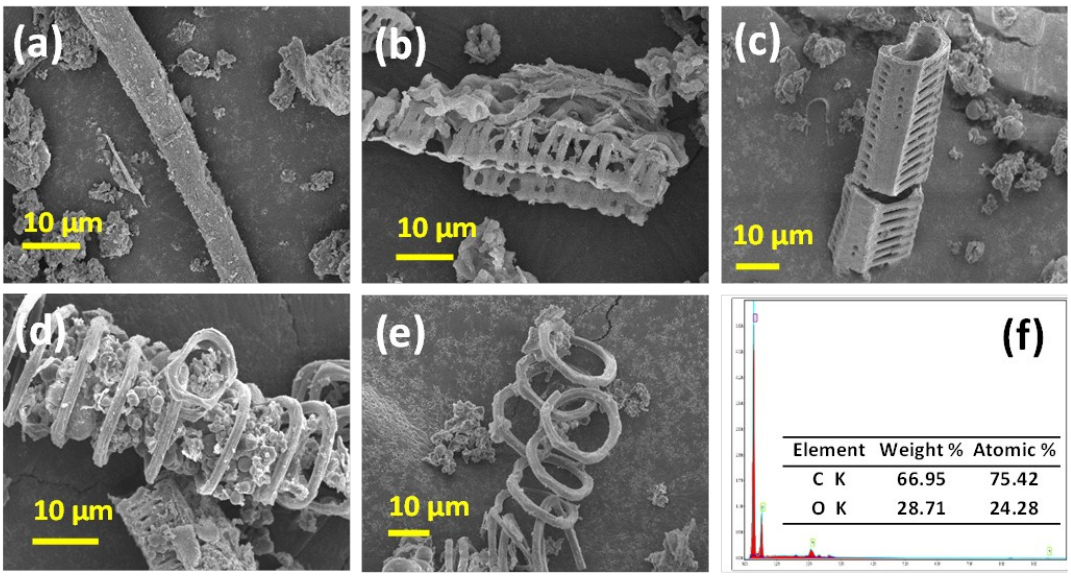

Figure S2. FESEM images of hydrothermally treated *Parthenium hysterophorous* using different mixtures of solvents (a) Control-CC (b) Control-Fe (c) PH-6-200 (d) PH-12-200 (e) PH-24-200 (f) Energy dispersive spectra (EDS) and Chemical composition (*inset*) of PH-18-200.

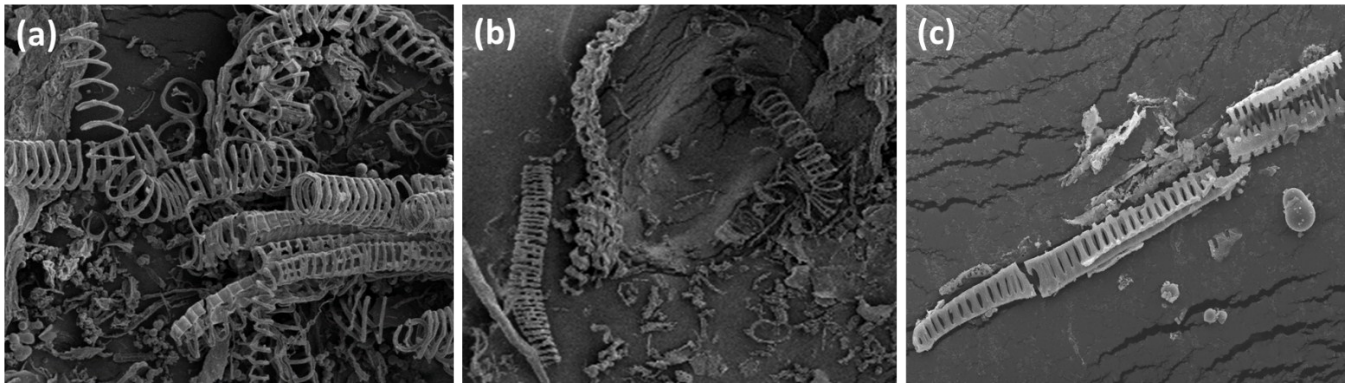

Figure S3. FESEM images of the carbon helices produced from *Parthenium hystrophorous* by recovered DES mixture. (a) 1st cycle, (b) 2nd cycle and (c) 3rd cycle.

Attenuated Total Reflection Infrared Spectroscopy (ATR-IR)

Attenuated total reflectance spectroscopy was used to analyze the presence of functional groups of samples prepared from different conditions (Figure S4 and S5). Peaks between 2930 cm^{-1} and 2810 cm^{-1} were associated to C-H stretching vibration in aliphatic and aromatic structures.[35] Peaks at 1703 cm^{-1} can be attributed to the stretching of C=O bonds, which are present in ketones, aldehydes, quinone, esters, and carboxylic acid functional groups.[36, 37] The vibration peaks at 1597.6 cm^{-1} and 1449.9 cm^{-1}, corresponding to the stretching of C=C groups, reflecting their aromatic groups.[35] The peak at 1207 cm^{-1} is attributed to the stretching of C–O bonds (carboxyl, ester, and ether groups).[38] The peaks in between 1460-1000 cm^{-1} are mainly attributed to C-O stretching vibrations.[39]

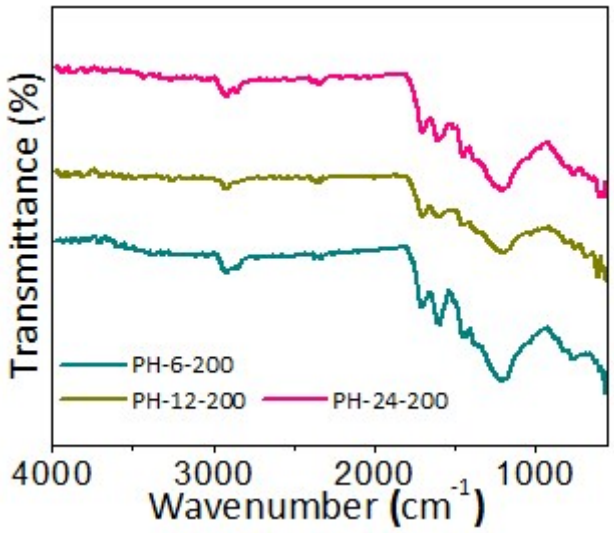

Figure S4. ATR-IR spectra of carbon helices prepared by hydrothermal method using different mixtures of solvents

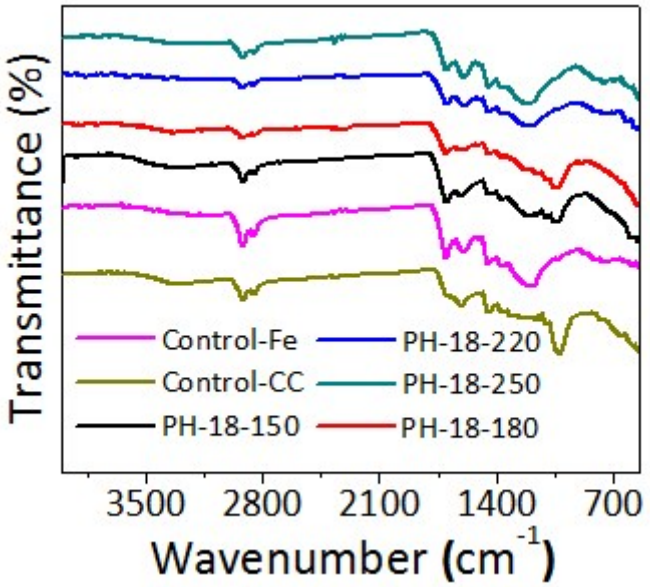

Figure S5. ATR-IR spectra of carbon helices prepared using hydrothermal method with different temperatures

Powder X-ray Diffraction

The crystal structure of the prepared samples analyzed using X-ray Diffraction. Figures S6 shows the p-XRD patterns of samples prepared from different conditions. For all the samples the major intensity peak at 26.68° corresponds to (111) hkl plane exactly matching with the JCPDS file-750444 which confirms the presence of carbon with rhombohedral crystal structure. A high intensity peak found at 21.32° showed the expansion of the lattice caused by the expansion of the cellulose matrix structure and the removal of hemicellulose during the process of solvothermal reaction.[8] The peaks appeared at the 2 theta of 28.0, 31.2 and 42.9 can be associated with (2 0 0), (4 0 0), (2 2 0) crystallographic planes respectively.[40] The crystal index of PH-18-150, Control-CC, and Control were 58.38%, 91.34%, and 60.00% respectively (Table S6).

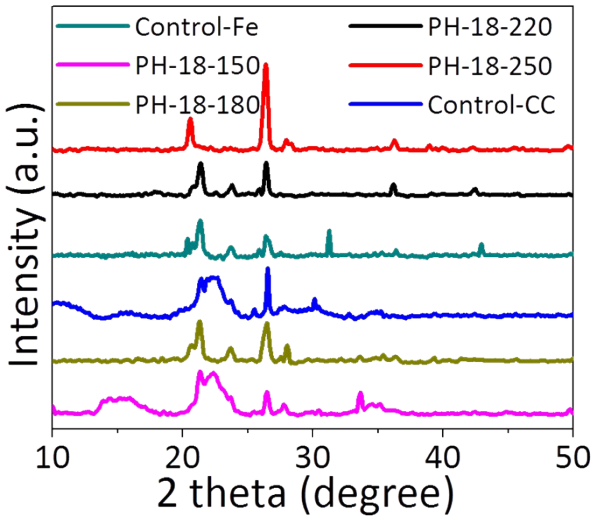

Figure S6. XRD patterns of carbon helices prepared by hydrothermal method at different conditions.

Table S6. Crystal index of prepared carbon helices under various conditions

Samples	Intensity at 2θ of 16° (A)	Intensity at 2θ of 22.1° (B)	Crystal Index (B-A)*100/B
PH-18-150	1047.57	2516.69	58.38
Control-CC	218.21	2520.63	91.34
Control	990.66	2476.49	60.00

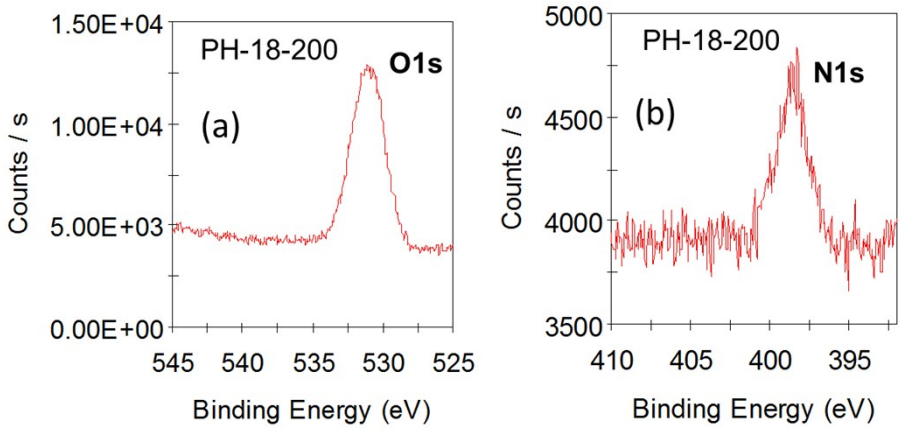

Figure S7. X-ray Photoelectron spectra of carbon helices prepared using hydrothermal method with different time duration

Mechanical property studies of material: Mechanical properties were studied by preparing k-carrageenan based films. The k-carrageenan, k-carrageenan + RC-18-200 and k-carrageenan + PH-18-200 films were prepared in the following way. Firstly the k-carrageenan (200 mg) was added in distilled water (10 mL), then mixture was heated at 70 °C, and stirred until the carrageenan was completely dissolved to give a clear and viscous solution. For the control film formation, 50 µL of glycerol added and kept at 70 °C for 5 minutes with continuous stirring. Then, the film was obtained by casting this viscous solution in petri-dish and kept at room temperature for overnight. Carrageenan + RC-18-200 and Carrageenan + PH-18-200 films were prepared with addition of RC-18-200 /PH-18-200 powder (5mg to 10mg) in carrageenan solution was dispersed by sonication for 10 min, afterwards this solution was again stirred at 70 °C for 30 minutes in order to ensure complete homogeneous solution. Furthermore homogeneous solution was cast in petri-dish and kept at room temperature for overnight to obtain a stable dry film (Figure S8A).

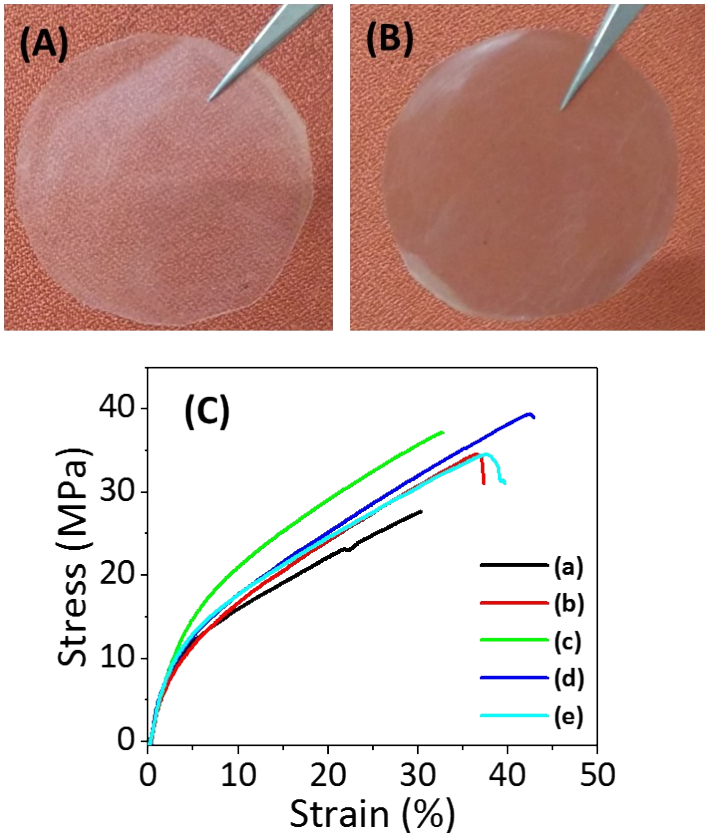

Figure S8. (A) Photograph of k-carrageenan film k-carrageenan composite film with 0.05 % (w/v) PH-18-200. (B) Plot of strain vs stress of different carbon materials prepared using different biomass (a) k-carrageenan (b) k-carrageenan + 0.05% (w/v) RC-18-200 (c) k-carrageenan + 0.1% (w/v) RC-18-200 (d) k-carrageenan + 0.05% (w/v) PH-18-200 (e) k-carrageenan + 0.1% (w/v) PH-18-200

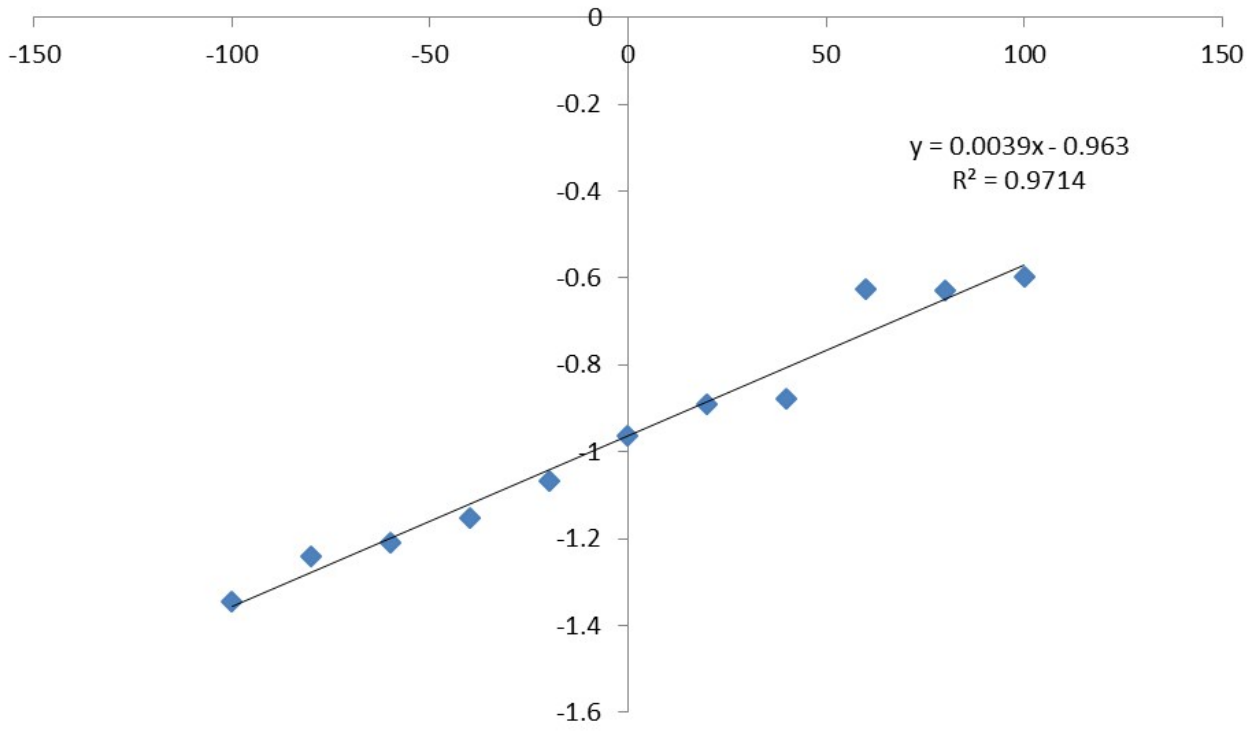

Figure S9. I-V plot of PH-18-200

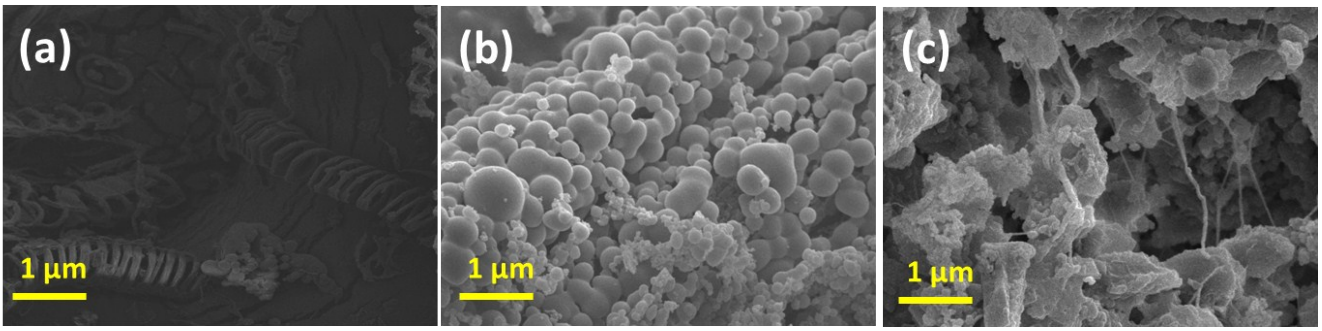

Figure S10. FESEM images of solvothermal carbon materials of (a) RC-18-200 (b) Cotton-18-200 and (c) BM-18-200

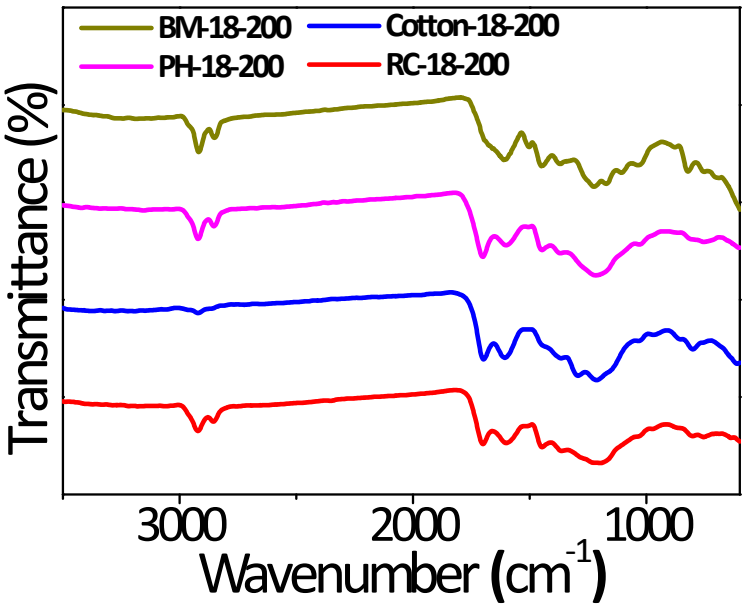

Figure S11. ATR-IR spectra of carbon materials prepared using different biomass.

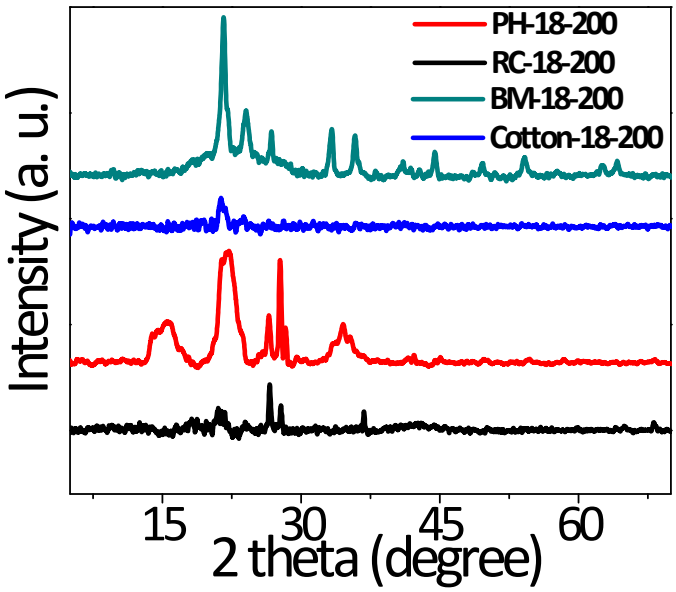

Figure S12. XRD spectra of carbon materials prepared using different biomass.

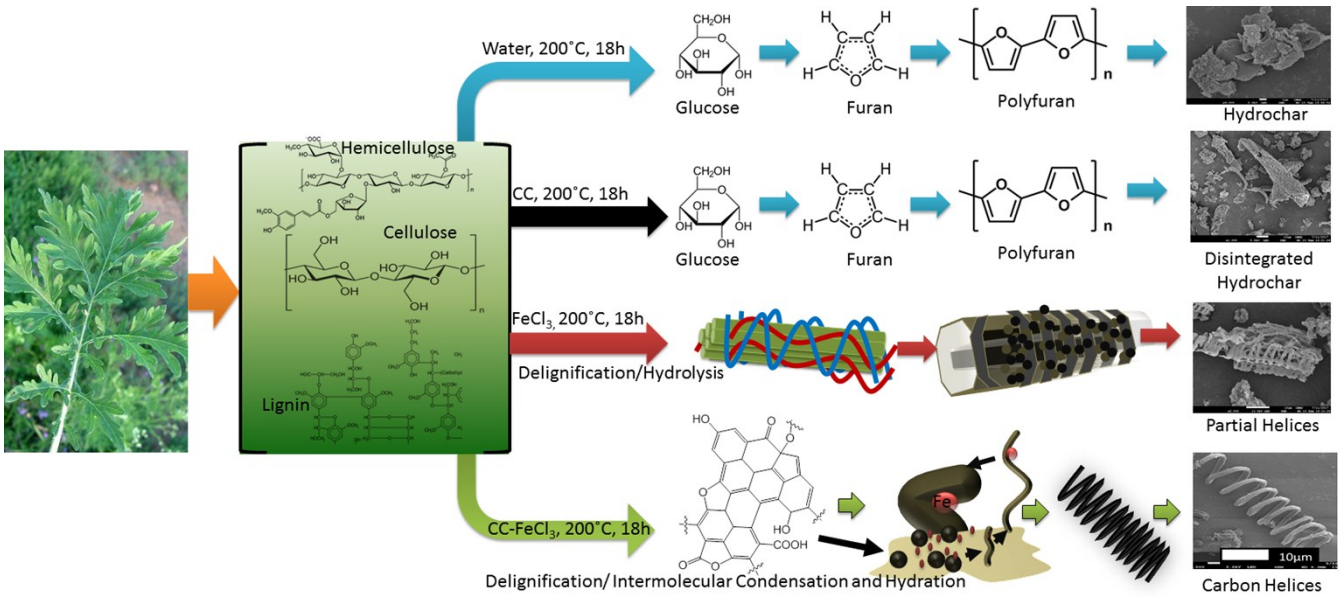

Figure S13: Schematics depiction of overall catalytic cycles to convert lignocellulosic biomass to solvothermal carbon with various morphologies under different reaction conditions.

Different potential supports for Cyt C and their limitations

In recent years, the applications of enzymes are increased in various fields such as fine-chemical synthesis, pharmaceutical chemistry, biofuel cells, wastewater bioremediation, fabrication of high performance biosensors, food processing, and protein digestion in proteomic analysis.[41 42 43 44 45] Enzymes are green catalysts, exhibit a high catalytic activity and selectivity without the need to work at harsh environment conditions such as high temperature, high pressure, and presence of organic solvents.[46] For commercial production, the use of enzymes limited due to high cost associated with the production and purification, low stability and loss of activity in change of environmental conditions, and the impossibility for reuse.[47] To overcome this limitations proper immobilization is required via multipoint attachment and generation of favorable enzyme environments to enrich the reusability and activity by attaching a support material with the enzyme.[48] The characteristics of a good support material includes inertness, physical strength, stability, regenerability, reduce product inhibition, and nonspecific adsorption.[49] Immobilization can be attained through two steps, (1) the multiple-point attachment to the support to restrict the structural changes of the enzyme in harsh environments, (2) Using insoluble support to enhance the recycle capacity of the enzyme.[50] So far many materials have been used as supports such as polymers, mesoporous silica, gold, diamond, graphene, nanotubes, and nanofibers, because of their ideal key factors such as mass transfer resistance, effective enzyme loading. Among these supports, carbon-based nanomaterials such as carbon nanotubes and graphene have attracted considerable interest for their significant advantages such as biocompatibility, highly developed pores, low cost and chemical stability.[51 52] The difference in graphene oxide (GO) and CNTs, GO decorated abundantly with functional groups where CNTs needs further functionalization. [53] Nevertheless, the preparation of GO requires harsh environments and expensive processes,[54] on the other hand after the functionalization also CNTs surface chemistry can affect the dispersability and the biological activity of the immobilized enzymes.[55] The functional groups such as hydroxyl, carboxylic and epoxides are efficient for immobilization of matrix. Therefore, in case of non-functionalized materials such as CNTs chemical functionalization is an important factor for grafting desirable functional groups onto the surface to obtain carbon materials with desired properties. **In the present study, tendril-like carbon helices have been prepared wherein the abundance functionalities present in biomass partly retained in final oxygenated carbon helices and thereby a win-win situation is created to immobilize Cyt C without compromising the activity and stability of the enzyme. Figure S14 shows the FESEM images of the protein immobilized carbon helices.**

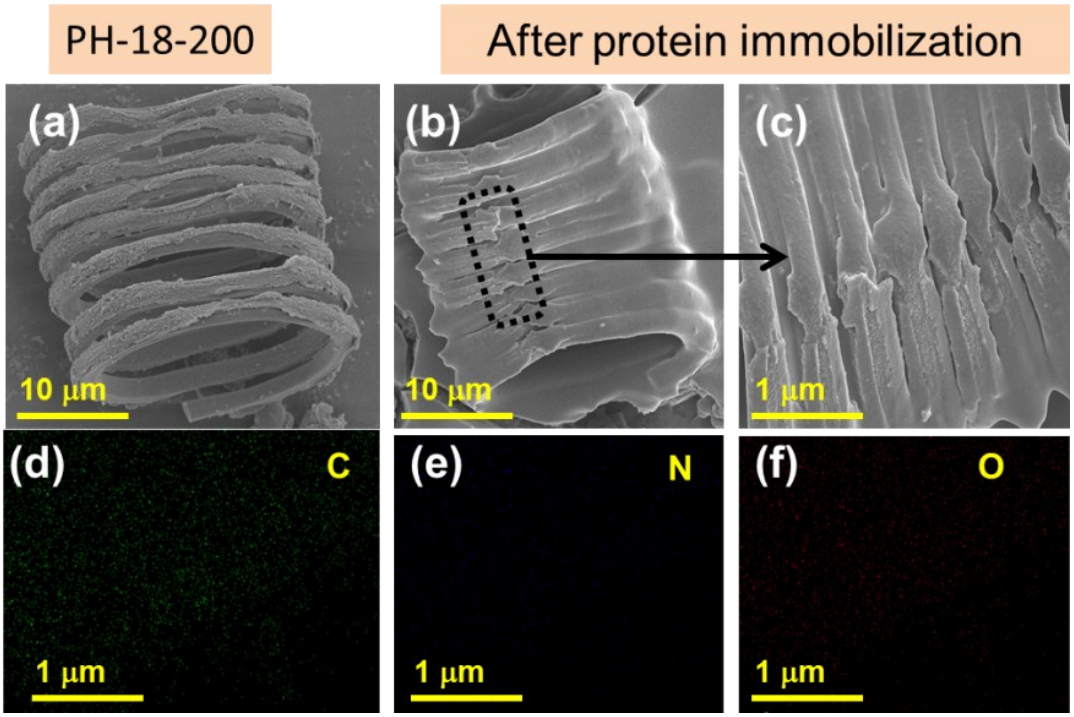

Figure S14: FESESM images of (a) PH-18-200 before protein immobilization, (b) after immobilization of Cyt C on PH-18-200, (c) higher magnification image of (b), (d) elemental mapping of C (green color), (e) elemental mapping of N (blue color) and (f) elemental mapping of O (red color)

Effect of carbon helices on the activity and stability of Cyt C

We have explored the influence of different carbon helices on the conformational activity and stability of Cyt C using UV-visible spectroscopy, Circular dichroism (CD) spectroscopy and FTIR measurements. The effect of different carbon on activity of Cyt C was determined using ABTS as substrate in presence of carbon material as discussed in previous report.[56]

UV-vis absorption spectra investigations of Cyt C in the presence of carbon helices

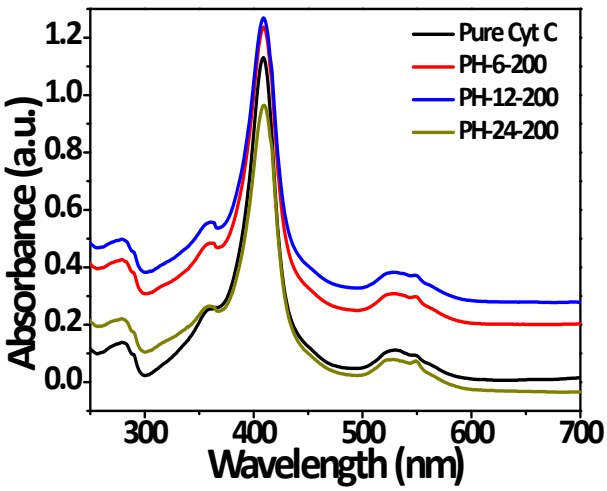

Figure S15. UV-Visible spectra of Cyt C in the presence of carbon helices

UV-vis spectroscopy is one of the most commonly applied spectroscopic technique for analyzing the conformational changes in the protein structure.[57, 58] Due to the presence of the heme prosthetic group, Cyt C shows some characteristic absorption bands. As displayed in Figure S15. Cyt C shows characteristic bands at ~ 280 nm, an intense Soret band around 409 nm, Q band at 528 and 550 nm. Our results are in good agreement with previous reports.[59] From the Figure S15, it is evident that there is insignificant shift in wavelength maxima (λ_{max}) of Cyt C in presence of aqueous solution of different solvothermal carbons, which indicates that carbon did not affect the polypeptide environment around the heme group and maintain the structure integrity of enzyme. However, the increase/decrease in the absorbance values can be due to absorbance of different carbon at 420 nm also due to some interactions occurring between the enzyme and solvothermal carbon.

FTIR Spectra of Cyt C in the presence of carbon helices

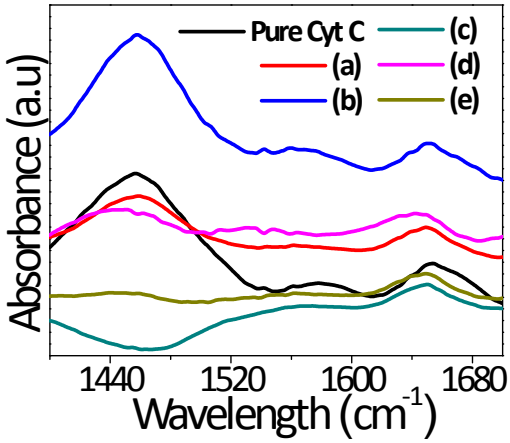

Figure S16. FTIR spectra of Cyt C in the presence of carbon helices in D_2O (a) PH-18-150 (b) PH-18-180 (c) PH-18-200 (d) PH-18-220 (e) PH-18-250

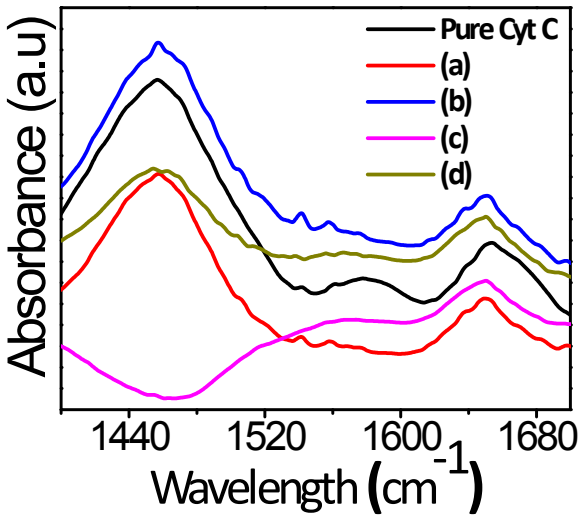

Figure S17. FTIR spectra of Cyt C in the presence of carbon helices in D_2O (a) PH-6-200 (b) PH-12-200 (c) PH-18-200 (d) PH-24-200

Figures S16 and S17 elucidates FTIR spectra which reveal gives information about the secondary structure of Cyt C in the presence of different solvothermal carbons. The amide I and amide II bands are very sensitive to the protein secondary structure.[60] Therefore, any conformational changes in the secondary structure of protein cause disturbance in the amide I and amide II regions in the FTIR spectra of the enzyme. Amide I band of protein is primarily related to the C=O stretching vibration of peptide backbone conformation, and amide II mainly corresponding to the N-H bending vibration and the C-N stretching vibration of the peptide backbone.[61] FTIR spectra of Cyt C in D_2O typically show two bands, amide I between 1700 and 1600 cm^{-1} and amide II between 1500 and 1400 cm^{-1}. The amide I band at 1650 cm^{-1} and amide II band at 1457 cm^{-1} for Cyt C in D_2O which is consistent with earlier reports.[60, 61] In D_2O solution the accessible N-H groups undergoes H-D exchange and there will be a small shift of amide I band and a large shift of the amide II band as compare to the H_2O.[61] In aqueous solutions of solvothermal carbons, there is no change in the amide I band, and amide II except the samples PH-18-200 and PH-18-250 which is due to the absorbance of pure carbon. Therefore, from FTIR results it is evident that all solvothermal carbons are able to keep Cyt C in its native form.

Circular Dichroism spectroscopic studies of Cyt C in the presence of carbon helices

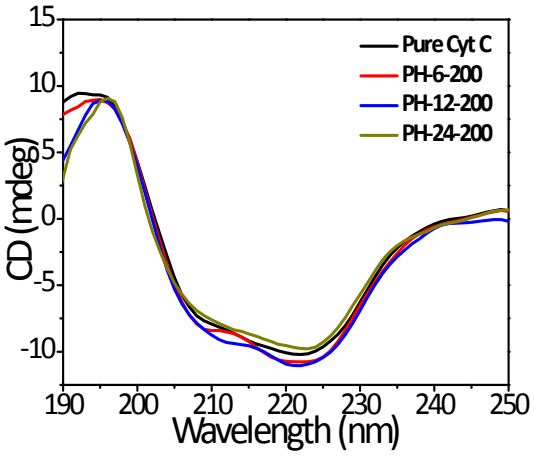

Figure S18. Far CD spectra of Cyt C in the presence of carbon helices in aqueous solutions

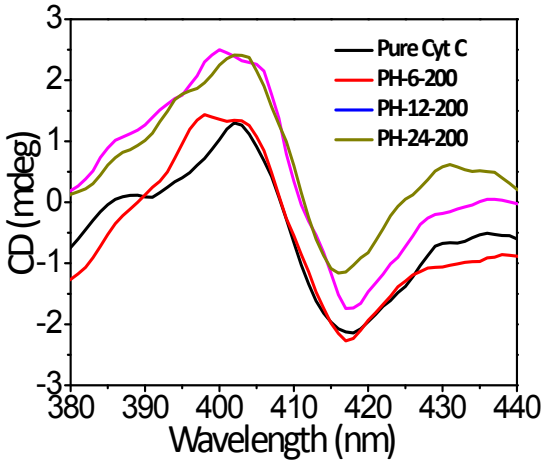

Figure S19. Near CD spectra of Cyt C in the presence of carbon helices in aqueous solutions

Further to explore the changes in the secondary and tertiary structure of Cyt C in presence of carbon, CD spectra were monitored and results are illustrated in Figures S18 and S19. Native Cyt C exhibits two negative maxima at 220 and 208 nm in far-UV CD region (190-250nm).[59] The soret region (350-450nm) spectra of Cyt C which provide further insight into tertiary structural changes is shown in Figure S15. Aqueous solution of Cyt C exhibits an intense positive band at ~406 nm and a strong negative band around ~416 nm.[62] The negative CD band around 416 nm is related to the presence of Met 80 at the sixth coordination position of the Cyt C.[56, 59, 62] As can be seen in Figure S19, after addition of solvothermal carbons there is no shift in bands position which shows no change near the porphyrin and heme vicinity. There is only slight change in intensity of positive band and negative band which suggest that incubation of Cyt C in aqueous solutions of solvothermal carbons did not affect conformation of the Cyt C.

References

1. H. C. Evans, *Biocontrol News and Information*, 1997, **18**, 89N-98N.
2. H. P. Singh, D. R. Batish, J. K. Pandher and R. K. Kohli, *Weed Biology and Management*, 2005, **5**, 105-109.
3. H. Lata, V. Garg and R. Gupta, *Journal of hazardous materials*, 2008, **157**, 503-509.
4. V. Subburam, *Bioresource technology*, 2002, **85**, 205-206.
5. M. Ajmal, R. A. K. Rao, R. Ahmad and M. A. Khan, *Journal of hazardous materials*, 2006, **135**, 242-248.
6. M.-M. Titirici, A. Funke and A. Kruse, in *Recent Advances in Thermo-Chemical Conversion of Biomass*, Elsevier, 2015, pp. 325-352.
7. D. Mondal, M. Sharma, C.-H. Wang, Y.-C. Lin, H.-C. Huang, A. Saha, S. K. Nataraj and K. Prasad, *Green Chemistry*, 2016, **18**, 2819-2826.
8. X. Ouyang, W. Wang, Q. Yuan, S. Li, Q. Zhang and P. Zhao, *RSC Advances*, 2015, **5**, 61650-61656.
9. Y. Lifshitz, G. Lempert and E. Grossman, *Physical review letters*, 1994, **72**, 2753.
10. M. F. De Volder, S. H. Tawfick, R. H. Baughman and A. J. Hart, *Science*, 2013, **339**, 535-539.
11. M. Ghosh, S. K. Sonkar, M. Saxena and S. Sarkar, *Small*, 2011, **7**, 3170-3177.
12. M. S. Mauter and M. Elimelech, *Environmental Science & Technology*, 2008, **42**, 5843-5859.

13. T. Ohba, K. Murata, K. Kaneko, W. Steele, F. Kokai, K. Takahashi, D. Kasuya, M. Yudasaka and S. Iijima, *Nano Letters*, 2001, **1**, 371-373.
14. K. P. De Jong and J. W. Geus, *Catalysis Reviews*, 2000, **42**, 481-510.
15. Y. Qin, Z. Zhang and Z. Cui, *Carbon*, 2004, **42**, 1917-1922.
16. Y. Zhai, Y. Dou, D. Zhao, P. F. Fulvio, R. T. Mayes and S. Dai, *Advanced materials*, 2011, **23**, 4828-4850.
17. M. A. Shannon, P. W. Bohn, M. Elimelech, J. G. Georgiadis, B. J. Marinas and A. M. Mayes, *Nature*, 2008, **452**, 301.
18. D. W. Wang, F. Li, M. Liu, G. Q. Lu and H. M. Cheng, *Angewandte Chemie*, 2008, **120**, 379-382.
19. G. Marland, T. O. West, B. Schlamadinger and L. Canella, *Tellus B*, 2003, **55**, 613-621.
20. G. Wang, Z. Gao, S. Tang, C. Chen, F. Duan, S. Zhao, S. Lin, Y. Feng, L. Zhou and Y. Qin, *ACS nano*, 2012, **6**, 11009-11017.
21. C. Li, L. Pan, C. Deng, P. Wang, Y. Huang and H. Nasir, *Nanoscale*, 2017, **9**, 9872-9878.
22. J. Deng, Y. Xu, S. He, P. Chen, L. Bao, Y. Hu, B. Wang, X. Sun and H. Peng, *nature protocols*, 2017, **12**, 1349.
23. J. F. AuBuchon, L.-H. Chen, A. I. Gapin, D.-W. Kim, C. Daraio and S. Jin, *Nano Letters*, 2004, **4**, 1781-1784.
24. K. Hirahara and Y. Nakayama, *Carbon*, 2013, **56**, 264-270.
25. N. Tang, W. Kuo, C. Jeng, L. Wang, K. Lin and Y. Du, *ACS nano*, 2010, **4**, 781-788.
26. X. Jian, M. Jiang, Z. Zhou, M. Yang, J. Lu, S. Hu, Y. Wang and D. Hui, *Carbon*, 2010, **48**, 4535-4541.
27. W.-C. Liu, H.-K. Lin, Y.-L. Chen, C.-Y. Lee and H.-T. Chiu, *Acs Nano*, 2010, **4**, 4149-4157.
28. Y. Qin, Y. Zhang and X. Sun, *Microchimica Acta*, 2009, **164**, 425-430.
29. S. Motojima, S. Kagiya and H. Iwanaga, *Materials Science and Engineering: B*, 1995, **34**, 47-52.
30. M. J. Hanus and A. T. Harris, *Carbon*, 2010, **48**, 2989-2992.
31. N.-K. Chang and S.-H. Chang, *Carbon*, 2008, **46**, 1106-1109.
32. X. Fu, L. Pan, D. Li, N. Zhou and Y. Sun, *Carbon*, 2015, **93**, 361-369.
33. R.-L. Liu, P. Yu, Z.-M. Luo, X.-F. Bai, X.-Q. Li and Q. Fu, *Chemical Engineering Journal*, 2017, **315**, 437-447.
34. E.-X. Ding, J. Wang, H.-Z. Geng, W.-Y. Wang, Y. Wang, Z.-C. Zhang, Z.-J. Luo, H.-J. Yang, C.-X. Zou and J. Kang, *Scientific reports*, 2015, **5**, 11281.
35. L. Zhang, Q. Wang, B. Wang, G. Yang, L. A. Lucia and J. Chen, *Energy & Fuels*, 2015, **29**, 872-876.
36. P. Gao, Y. Zhou, F. Meng, Y. Zhang, Z. Liu, W. Zhang and G. Xue, *Energy*, 2016, **97**, 238-245.
37. A. Fuertes, M. C. Arbestain, M. Sevilla, J. A. Maciá-Agulló, S. Fiol, R. López, R. Smernik, W. Aitkenhead, F. Arce and F. Macìas, *Soil Research*, 2010, **48**, 618-626.
38. J. Torres, F. Nogueira, M. Silva, J. Lopes, T. Tavares, T. Ramalho and A. Corrêa, *RSC Advances*, 2017, **7**, 16460-16466.
39. E. P. Cipolatti, A. Valério, R. O. Henriques, D. E. Moritz, J. L. Ninow, D. M. Freire, E. A. Manoel, R. Fernandez-Lafuente and D. de Oliveira, *RSC Advances*, 2016, **6**, 104675-104692.
40. M. Salavati-Niasari and P. G. Sheikhiabadi, *Journal of Industrial and Engineering Chemistry*, 2014, **20**, 3793-3799.
41. R. D. Schmid and R. Verger, *Angewandte Chemie International Edition*, 1998, **37**, 1608-1633.
42. J. Thiem, *FEMS microbiology reviews*, 1995, **16**, 193-211.
43. N. Duran and E. Esposito, *Applied catalysis B: environmental*, 2000, **28**, 83-99.
44. M. Bhat and S. Bhat, *Biotechnology advances*, 1997, **15**, 583-620.
45. O. Bodansky, *The American journal of medicine*, 1959, **27**, 861-874.
46. G. Carrea and S. Riva, *Angewandte Chemie International Edition*, 2000, **39**, 2226-2254.
47. M. Hartmann and D. Jung, *Journal of Materials Chemistry*, 2010, **20**, 844-857.

48. C. Garcia‐Galan, Á. Berenguer‐Murcia, R. Fernandez‐Lafuente and R. C. Rodrigues, *Advanced Synthesis & Catalysis*, 2011, **353**, 2885-2904.
49. Y. Wang and F. Caruso, *Chemistry of Materials*, 2005, **17**, 953-961.
50. S. A. Ansari and Q. Husain, *Biotechnology advances*, 2012, **30**, 512-523.
51. A. Zebda, C. Gondran, A. Le Goff, M. Holzinger, P. Cinquin and S. Cosnier, *Nature communications*, 2011, **2**, 370.
52. K. Besteman, J.-O. Lee, F. G. Wiertz, H. A. Heering and C. Dekker, *Nano letters*, 2003, **3**, 727-730.
53. A. Hirsch and O. Vostrowsky, in *Functional molecular nanostructures*, Springer, 2005, pp. 193-237.
54. L. Chen, Y. Hernandez, X. Feng and K. Müllen, *Angewandte Chemie International Edition*, 2012, **51**, 7640-7654.
55. W. Feng and P. Ji, *Biotechnology advances*, 2011, **29**, 889-895.
56. M. Bisht, D. Mondal, M. M. Pereira, M. G. Freire, P. Venkatesu and J. Coutinho, *Green Chemistry*, 2017.
57. S. Oellerich, H. Wackerbarth and P. Hildebrandt, *European Biophysics Journal*, 2003, **32**, 599-613.
58. P. Bharmoria, T. J. Trivedi, A. Pabbathi, A. Samanta and A. Kumar, *Physical Chemistry Chemical Physics*, 2015, **17**, 10189-10199.
59. R. Santucci and F. Ascoli, *Journal of inorganic biochemistry*, 1997, **68**, 211-214.
60. A. Dong, P. Huang and W. S. Caughey, *Biochemistry*, 1992, **31**, 182-189.
61. T. Heimburg and D. Marsh, *Biophysical journal*, 1993, **65**, 2408-2417.
62. G. Blauer, N. Sreerama and R. W. Woody, *Biochemistry*, 1993, **32**, 6674-6679.